

Parametric Study of Dry Sliding Wear Behavior of Hybrid Metal Matrix Composite Produced by a Novel Process



PARDEEP SHARMA, SATPAL SHARMA, and DINESH KHANDUJA

In the present research work, silicon nitride (Si_3N_4) and graphite (Gr) ceramic powders are ball milled to obtain homogeneous mixing and consistent density of combined powder. The ball-milled powder is used as reinforcement for hybrid composite development by stir casting process in the inert atmosphere. After mixing by ball milling for 100 hours, the density of ball-milled ($\text{Si}_3\text{N}_4 + \text{Gr}$) powder is measured as 2.81 g/cm^3 , which is approximately equal to the density of aluminum (2.7 g/cm^3). The microstructures and hardness of the manufactured hybrid composites are analyzed and compared with Si_3N_4 - and Gr-reinforced composites. Scanning electron micrograph reveals a reasonably uniform dispersion of ball-milled ($\text{Si}_3\text{N}_4 + \text{Gr}$) reinforcement in the metal matrix composites. Hardness results reveal that hybrid composites have more hardness than Gr-reinforced and lower hardness than Si_3N_4 -reinforced composites. The dry sliding wear behavior of aluminum matrix hybrid composites has also been investigated. Response surface methodology is used to develop wear model of hybrid composites using reinforcement percentage (R), load (L), sliding speed (S), and sliding distance (D) as the process parameters. The results of wear investigation show that increase in sliding speed (S) and percentage reinforcement (R) reduce the wear, while increase in sliding distance (D) or load (L) increases the wear of the hybrid composites. Further, the load-sliding distance and load-sliding speed interactions increase the wear, while the wear reduces due to sliding speed-sliding distance interaction in the high range. The errors between the modeled and experimental results are found within 3 to 7 pct.

DOI: 10.1007/s11661-015-2881-9

© The Minerals, Metals & Materials Society and ASM International 2015

I. INTRODUCTION

IN recent times, the aluminum matrix composites (AMCs) due to their better mechanical and tribological properties found increasing applications than conventional aluminum alloys. The AMCs are formed with the addition of various types of reinforcements such as graphite, silicon carbide, silicon nitride, aluminum oxide, *etc.*, with advantages and disadvantages of each type of reinforcement in the metal matrix. Graphite (Gr), a self-lubricating material, prevents metal-to-metal contact by forming a thin layer of Gr particle, therefore Al-Gr composites have better wear resistance than conventional aluminum alloy. Liu *et al.*^[1] showed that in Al-Gr composites, Gr formed a thin lubricating film which significantly improved the wear resistance of composites. Various researchers^[2-4] showed that an increase in Gr content reduced the coefficient of friction, hardness, and fracture toughness of composites developed by various fabrication processes. All these studies showed that Al-Gr composites had reduced wear

as compared to conventional aluminum alloy, but high amount of Gr may result in increased wear because of reduced fracture toughness at higher content of Gr.^[4]

The mechanical properties of Si_3N_4 and SiC are similar but Si_3N_4 is harder than SiC. The Si_3N_4 can be used in place of SiC in order to develop more hard AMCs, while the Gr as a second reinforcement provides the lubricating effect to reduce friction and wear. Various researchers^[5-10] showed that addition of silicon nitride (Si_3N_4) in aluminum matrix for composite development resulted in high mechanical strength, high hardness, good wear and corrosion resistance, low thermal expansion, high specific strength, thermal conductivity, and good dimensional stability. Hence, addition of Si_3N_4 particulates improved both the mechanical and tribological properties of aluminum alloy.

But the addition of Gr in Al-Gr composites and Si_3N_4 in Al- Si_3N_4 composites is constrained by definite inadequacy beyond which it is not favorable to add either higher concentration of Gr or Si_3N_4 as reinforcement. Thus, it would be beneficial to reinforce Si_3N_4 and Gr together in aluminum (Al) alloy to develop hybrid composites. The prominent outcome of some studies on hybrid aluminum matrix composites (HAMCs) is briefed in the next few lines.

Some researchers^[11-16] showed that Al-SiC-Gr hybrid composites possessed higher hardness, and their wear resistance increased by adding SiC as second reinforce-

PARDEEP SHARMA, PhD Research Scholar, and DINESH KHANDUJA, Professor, are with the Mechanical Engineering Department, National Institute of Technology Kurukshetra, Kurukshetra 136118, Haryana, India. Contact e-mail: pardeep84sharma@gmail.com SATPAL SHARMA, Assistant Professor, is with the Mechanical Engineering Department, School of Engineering, Gautam Buddha University, Greater Noida 201306, Uttar Pradesh, India.

Manuscript submitted December 18, 2014.

Article published online April 4, 2015

ment. Studies on hybrid composites of similar type showed that hardness and coefficient of thermal expansion (CTE) of the composites decreased as the Gr content increased.^[4] Rohatgi *et al.*^[13] reported that the reduction in friction coefficient of Al-10SiC-6Gr was due to the combination of increase in bulk mechanical properties as a result of addition of SiC and formation of lubricating Gr film. Alidokht *et al.*^[15] showed that the incorporation of silicon carbide particulates (SiCp) to A356 alloy increased the wear resistance of the composites, and the wear resistance of hybrid composite was further increased with the addition of MoS₂ as second reinforcement in A356/SiCp composites. Thus, hybrid composites with multiple reinforcements possessed better tribological properties than conventional aluminum alloy and single reinforced composites as reported in the above investigations.

AA6082 is a transitional strength alloy of the 6XXX series with fantastic corrosion resistance. The amount of manganese present in AA6082 controls the grain structure which results into a strong and hard alloy. The amount of silicon is high in AA6082 which increases its wear resistance, and it finds applications in the arena of bridges, trusses, high strain application and in the manufacturing of automobile components. Due to its good wear and corrosion resistance, it can be used in tribological applications and can replace the prevailing materials in the production of hydraulic brake system components, like brake piston, where high wear resistance material is of primary concern. So AA 6082 is selected as a metal matrix for hybrid composite development. The application of the alloy can be further extended if the tribological properties of the present alloy have been improved since it has good corrosion resistance. In view of the above facts in the present investigation, an attempt has been made to study the dry sliding wear properties of Al6082/ball-milled (Si₃N₄ + Gr) hybrid composites developed by stir casting process.

Different investigators^[17–19] had examined the wear behavior of AMCs by response surface methodology (RSM) technique and convey that the effect of interaction among different process variable is low, still cannot be neglected to obtain the better results. But in the past, a vast amount of data had been generated by the traditional approach of experiments in which one factor was varied at a time (load, sliding speed, *etc.*). In this approach, it was difficult to evaluate the combined effects of applied factors.^[20] Thus, RSM with full factorial design of experiments, with five levels of each factor, has been used in the present study (rotatable central composite design). In this technique, the effect of individual process parameters along with the interaction

effects of process parameters can be investigated to understand the overall effects of different process parameters on dry sliding wear of the developed hybrid composites. This research provides the range of different process parameters like reinforcement percentage, load, sliding speed, and sliding distance to obtain the better results from the new material developed, which will help the automotive researchers to use this new material in tribological applications.

II. RESEARCH METHODOLOGY

A. Ball Milling for Homogeneous Mixing of Reinforcements

Silicon nitride (purity > 99 pct) and graphite (purity > 99 pct) of composition of 50 wt pct of each reinforcement were alloyed mechanically by ball milling in an attritor-type ball mill, using ceramic balls of 6 and 9 mm diameter as the grinding media. The ball milling was carried out with different milling times of 12.5, 25, 50, 75, and 100 hours under a protective atmosphere to avoid oxidation and atmospheric contamination of ceramic powders. Ball-to-powder weight ratio (BPR) of 5:1 and constant milling speed of 200 rpm was maintained during ball-milling process.

B. Development of Composites by Stir Casting Process

The hybrid composites were developed for the mechanical and tribological analysis using AA 6082 and ball-milled (Si₃N₄ + Gr) reinforcement by stir casting process. The composition of matrix alloy AA 6082-T6 is shown in Table I, while Table II provides the details of Si₃N₄ and Gr reinforcements. 1 kg of aluminum alloy by weight was measured and put in the graphite crucible and was melted at 1173 K (900 °C) using an electric furnace. The ball-milled (Si₃N₄ + Gr) ceramic powder was also preheated to a temperature of 773 K (500 °C). The preheated ball-milled powder was added at a constant feed rate into the melt which was mechanically stirred for 10 minutes.^[21,22] After stirring the molten mixture, it was poured into the preheated permanent

Table II. Details of Reinforcements Used in Production of Hybrid Composites

Reinforcement	Hardness (Gpa)	Average Particle Size (μm)	Density (g/cm ³)
Si ₃ N ₄	35.31	50	3.44
Gr	0.25	50	2.2

Table I. Chemical Composition of AA6082-T6

Element	Al	Cu	Mg	Si	Fe	Ni	Mn
Content percent	97.14	0.038	0.690	1.16	0.258	0.04	0.580
Element	Zn	Pb	Tin	Ti	Cr	Vn	
Content percent	0.027	<0.001	0.006	0.048	0.042	<0.01	

mold of dimension 12 mm diameter and 55 mm length. The hybrid aluminum matrix composites (HAMCs) having different weight percentages (3, 6, 9, 12 wt pct) of ball-milled ($\text{Si}_3\text{N}_4 + \text{Gr}$) ceramic powders were manufactured by the same procedure. The stir casting process was performed under argon gas atmosphere until the entire melt was solidified.

C. Microstructural Study

A metallographic study of Si_3N_4 , Gr and ball-milled ($\text{Si}_3\text{N}_4 + \text{Gr}$) reinforced composites was carried out using scanning electron microscope (SEM). Before SEM analysis, the samples were prepared from developed hybrid composites and polished by adopting standard metallographic procedure and etched using Keller's etchant.

D. Hardness Measurement

A micro-hardness study of Si_3N_4 , Gr and ball-milled ($\text{Si}_3\text{N}_4 + \text{Gr}$) reinforced composites was carried out using Vickers hardness tester at a load of 500 g applied for a duration of 15 seconds on all specimens. Table III shows the average Vickers hardness of composites as a function of different weight percentages.

E. Wear Test

Wear test samples of dimension, diameter of 8 mm and length of 35 mm, were prepared from the manufactured hybrid composites. The wear tests were performed on pin-on-disk apparatus. The counter disk was made of EN31 steel having surface roughness of $0.1 \mu\text{m}$. The wear was measured by weight loss, as a difference of weights of the wear pins, before and after wear tests to an accuracy of 0.0001 g.

F. Response Surface Methodology

Applied load and hardness greatly influence the wear of materials.^[23] The hardness is the material

property which depends upon the type of reinforcement in AMCs. In view of these facts, the load and percentage reinforcement were taken as process parameters along with the sliding speed and sliding distance in this research. Hence, percentage reinforcement, load, sliding speed, and sliding distance were four process parameters used in the present study. These factors were designated as percentage reinforcement (R), load (L), sliding speed (S), and sliding distance (D), respectively. Response surface methodology with central composite design (CCD) was used to plan and analyze the design of experiments. The central composite design (CCD) contains factorial points each at upper (+1) and lower (-1) values, center points (0) and axial points of upper (+2) and lower (-2) values. In this way, there are five levels of each process parameters in CCD. Table IV shows the factors and their levels used in the present analysis. The experimental design matrix for various factors with their actual and coded values (in parentheses) has been shown in Table V.

The relation between the actual and coded value of a factor has been shown below:

$$\text{Coded value} = \frac{\text{Actual test conditions} - \text{Mean test conditions}}{\text{Range of test conditions}/2}$$

The wear tests were performed according to design matrix (Table V), and the weight loss was measured to evaluate the wear behavior Al- $(\text{Si}_3\text{N}_4 + \text{Gr})$ hybrid composites.

III. RESULTS AND DISCUSSION

A. Ball Milling of Reinforcement

The ball milling of reinforcement (Si_3N_4 and Gr) was carried out in order to get homogeneous mixture of

Table III. Average Vickers Hardness of Various Composites

Reinforcement (Weight Percent)	Hardness of Gr Reinforced Composites	Hardness of Si_3N_4 Reinforced Composites	Hardness of ($\text{Si}_3\text{N}_4 + \text{Gr}$) Reinforced Hybrid Composites
0	49.5	49.5	49.5
3	48	82	72
6	46.5	86	76
9	45.2	91	81
12	44	93.5	84

Table IV. Factors and Their Levels Used in CCD Experimental Plan

Factors	Designation	Levels				
		-2	-1	0	+1	+2
Reinforcement (wt pct)	R	0	3	6	9	12
Load (N)	L	15	30	45	60	75
Sliding speed (m/s)	S	0.4	0.8	1.2	1.6	2.0
Sliding distance (m)	D	400	800	1200	1600	2000

Table V. Details of Test Combinations with Their Actual and Coded Value (in Parentheses) and Corresponding Experimental Results

Run No.	Process Parameters				Wear Al-Si ₃ N ₄ -Gr (g)
	Reinforcement (R)	Load (L)	Sliding Speed (S)	Sliding Distance (D)	
1	3 (-1)	30 (-1)	0.8 (-1)	800 (-1)	0.0077
2	9 (+1)	30 (-1)	0.8 (-1)	800 (-1)	0.0061
3	3 (-1)	60 (+1)	0.8 (-1)	800 (-1)	0.0088
4	9 (+1)	60 (+1)	0.8 (-1)	800 (-1)	0.0065
5	3 (-1)	30 (-1)	1.6 (+1)	800 (-1)	0.0046
6	9 (+1)	30 (-1)	1.6 (+1)	800 (-1)	0.0024
7	3 (-1)	60 (+1)	1.6 (+1)	800 (-1)	0.0058
8	9 (+1)	60 (+1)	1.6 (+1)	800 (-1)	0.0048
9	3 (-1)	30 (-1)	0.8 (-1)	1600 (+1)	0.0162
10	9 (+1)	30 (-1)	0.8 (-1)	1600 (+1)	0.0146
11	3 (-1)	60 (+1)	0.8 (-1)	1600 (+1)	0.0186
12	9 (+1)	60 (+1)	0.8 (-1)	1600 (+1)	0.0174
13	3 (-1)	30 (-1)	1.6 (+1)	1600 (+1)	0.0095
14	9 (+1)	30 (-1)	1.6 (+1)	1600 (+1)	0.0083
15	3 (-1)	60 (+1)	1.6 (+1)	1600 (+1)	0.0154
16	9 (+1)	60 (+1)	1.6 (+1)	1600 (+1)	0.0132
17	0 (-2)	45 (0)	1.2 (0)	1200 (0)	0.012
18	12 (+2)	45 (0)	1.2 (0)	1200 (0)	0.0078
19	6 (0)	15 (-2)	1.2 (0)	1200 (0)	0.0054
20	6 (0)	75 (+2)	1.2 (0)	1200 (0)	0.01
21	6 (0)	45 (0)	0.4 (-2)	1200 (0)	0.0125
22	6 (0)	45 (0)	2 (+2)	1200 (0)	0.0076
23	6 (0)	45 (0)	1.2 (0)	400 (-2)	0.0018
24	6 (0)	45 (0)	1.2 (0)	2000 (+2)	0.02
25	6 (0)	45 (0)	1.2 (0)	1200 (0)	0.0086
26	6 (0)	45 (0)	1.2 (0)	1200 (0)	0.0082
27	6 (0)	45 (0)	1.2 (0)	1200 (0)	0.0087
28	6 (0)	45 (0)	1.2 (0)	1200 (0)	0.0085
29	6 (0)	45 (0)	1.2 (0)	1200 (0)	0.0077
30	6 (0)	45 (0)	1.2 (0)	1200 (0)	0.0089

reinforcements. During ball-milling process, extreme mechanical deformation takes place which causes the structural changes in the combined powder.^[24-26] Figures 1((a) through (f)) shows the SEM images of (Si₃N₄ + Gr) combined at various ball-milling times. From Figure 1(a), it is evident that the microstructure was not homogeneous at the start of milling process, and silicon nitride and graphite can be seen separately. The graphite particles were slightly white, while silicon nitride phase appeared dark in micrograph. During the initial period of ball milling, the powder particles were also non-homogeneous. After 25 hours of ball-milling process, the powder particles were in cold welding condition and appeared like inflated fragments (Figure 1(c)). These fragment-shaped combined particles were further crushed during ball milling which resulted in uniform mixing of powders as shown in Figures 1((e) and (f)). The final shape of the ball-milled powder was sub-angular and surface morphology was rough. After 100 hours of ball milling, it is revealed from the Figure 1(f) that structure was more homogeneous as compared to 0 hours of ball milling (Figure 1(a)). It might be due to proper mixing of silicon nitride and graphite particles by ball-milling process. With increasing milling time, the specific surface area of combined powder increased. This increase in surface area promoted van der Waals' interaction and high surface rough-

ness of combined ball-milled powders.^[27] This increase in surface roughness also promoted the increased wettability, which resulted into compatibility with metal matrices as in case of AMCs. Hence, the enhanced rough and unstructured phases are promising and advantageous as it may lead to more compatibility with metal matrices. The density of ball-milled powder after 100 hours was measured as 2.81 g/cm³, which was approximately equal to the density of aluminum (2.7 g/cm³).

B. Microstructure Analysis

Aluminum reinforced with Si₃N₄, Gr, and ball-milled (Si₃N₄ + Gr) ceramic particulate composites are successfully manufactured by conventional stir casting process. Figures 2((a) through (d)) shows the microstructures of cast AA6082 (0 pct reinforcement), AA6082/12 wt pct Si₃N₄-reinforced composite, AA6082/12 wt pct Gr-reinforced composite, and AA6082/12 wt pct (Si₃N₄ + Gr)-reinforced hybrid composites, respectively. The microstructure of cast Al 6082 consists of solid solution of aluminum and inter-dendritic network of aluminum silicon eutectic (Figure 2(a)). Figure 2(b) shows the SEM image of AMC reinforced with 12 wt pct of Si₃N₄. The SEM image reveals non-homogeneous distribution of Si₃N₄ ceramic particulates in the aluminum metal

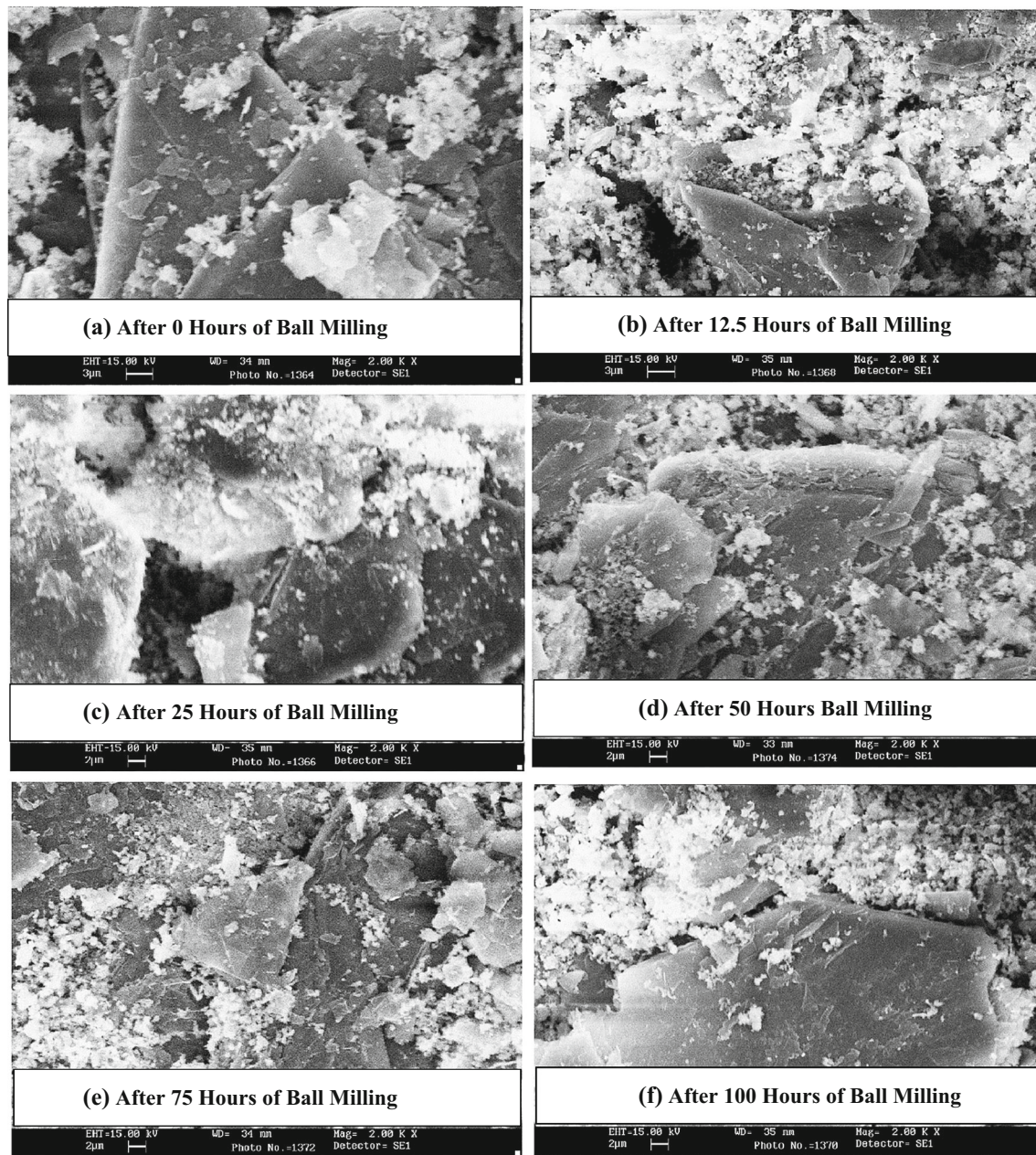


Fig. 1—SEM Micrograph of ball milled ($\text{Si}_3\text{N}_4 + \text{Gr}$) at various milling times (a) 0 h (b) 12.5 h (c) 25 h (d) 50 h (e) 75 h (f) 100 h.

matrix, which may be due to a large difference in densities of AA 6082 (2.7 g/cm^3) and Si_3N_4 reinforcement (3.44 g/cm^3) particles. Due to difference in densities, the heavier reinforcement particles try to sink down in the aluminum melt before complete solidification takes place. Similarly, Figure 2(c) shows the SEM image of AMC reinforced with 12 wt pct of Gr reinforcement. It is revealed from SEM image that there are large impurities with a non-uniform distribution of Gr particles. The low density (2.2 g/cm^3) of Gr particles as compared to that of AA 6082 (2.7 g/cm^3) causes the Gr particles to float in the aluminum melt resulting in non-uniform distribution. Proper distribution of reinforcement particles is a mandatory condition to enhance the mechanical properties of aluminum metal matrix composites. Figure 2(d) shows

the SEM image of AMC reinforced with 12 wt pct of ball-milled ($\text{Si}_3\text{N}_4 + \text{Gr}$) reinforcement. It is observed from SEM image that ball-milled ($\text{Si}_3\text{N}_4 + \text{Gr}$) ceramic particulates are dispersed uniformly in the aluminum matrix which may be due to approximately equal density (2.81 g/cm^3) of ball-milled ($\text{Si}_3\text{N}_4 + \text{Gr}$) reinforcement to that of Al (2.7 g/cm^3) causing the reinforcement particles to neither float nor sink down in the aluminum melt. SEM image of hybrid composite reveals a clear interface between metal matrix and reinforcement. In all the manufactured AMCs (Figures 2(a) through (d)), Mg_2Si precipitates are present, the source of which are magnesium and silicon present in the matrix. Out of the single reinforced and hybrid composites, a more uniform distribution has been achieved in the hybrid composite

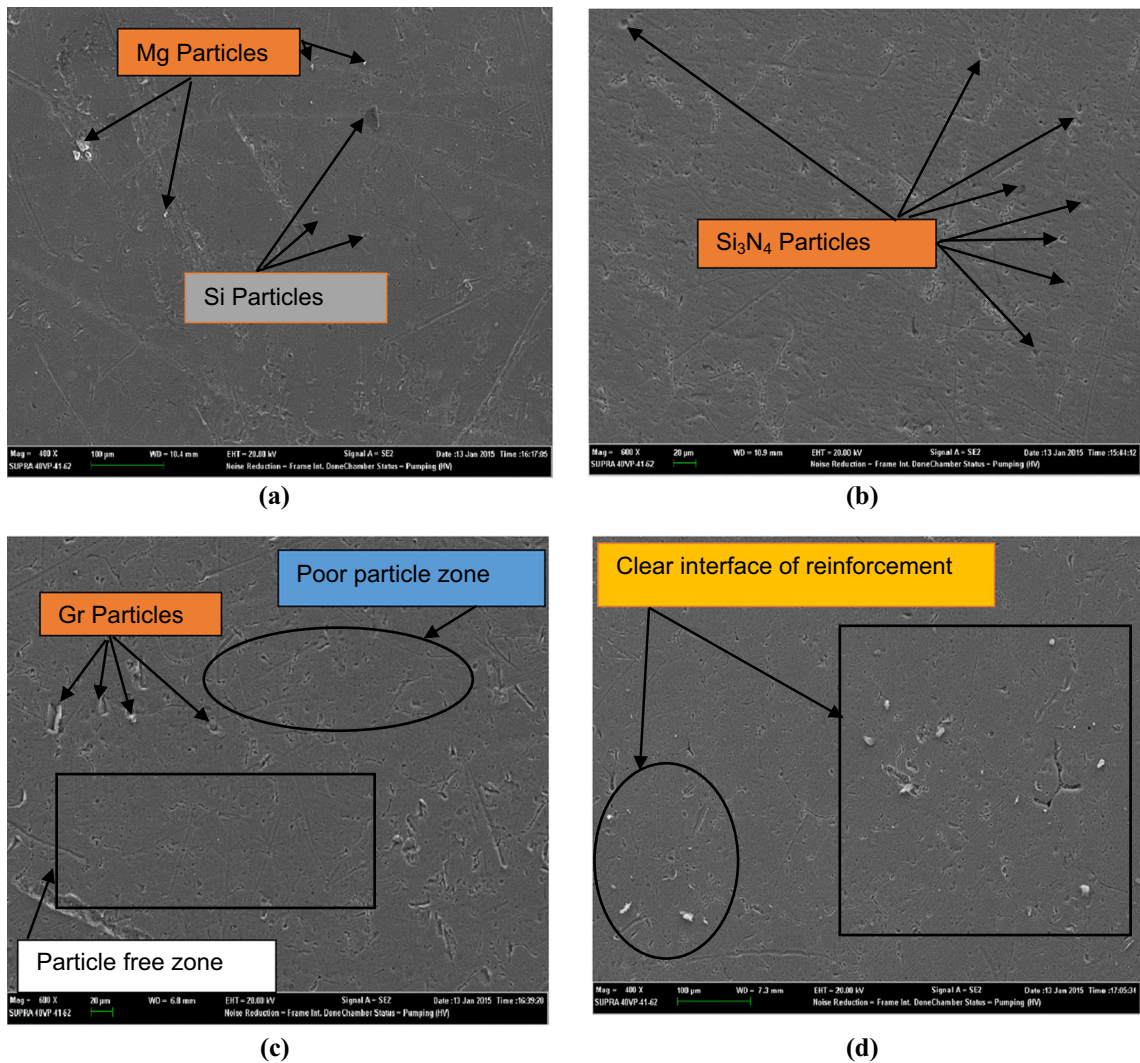


Fig. 2—SEM image of (a) cast AA6082 (0 wt pct reinforcement) (b) AA6082/12 wt pct Si_3N_4 -reinforced composite (c) AA6082/12 wt pct Gr-reinforced composite (d) AA6082/12 wt pct (Si_3N_4 + Gr)-reinforced hybrid composite.

which may be due to approximately equal density of combined reinforcement to that of aluminum metal matrix.

C. Hardness Result

Table III shows the average Vickers hardness of composites. The hardness of Gr-reinforced composites decreases with the increasing content of Gr, this may be due to low hardness of reinforcement particles than that of AA6082. At a high percentage of Gr, the reinforcement particles which are soft, float in large amount, and result in large impurities on the surface of the aluminum melt, due to which the impurity content increases which results in low hardness. Same trend of hardness was observed by previous researchers with the increasing content of Gr in AMCs regardless of the fabrication process of AMCs.^[2,3,14] In case of Si_3N_4 -reinforced composites, it is revealed that hardness of AMCs is increasing linearly with the increase in weight percentage of Si_3N_4 ceramic particulates. This may be attributed because of the increase in hard ceramic particles in the

alloy matrix and high hardness of reinforcement. The presence of these hard Si_3N_4 ceramic particulates offers large resistance to the plastic deformation which results into enhancement of the hardness of manufactured AMCs. Same results of increase in hardness with increasing content of Si_3N_4 reinforcement in the metal matrix composites irrespective of the manufacturing process of AMCs were obtained by former investigators.^[6–8] The hardness of hybrid composites also shows an increasing trend with the increased content of ball-milled (Si_3N_4 + Gr) ceramic particulates in the metal matrix. This may be due to the presence of hard and brittle (Si_3N_4 + Gr) ceramic particulates in the soft and ductile AA6082 metal matrix which reduces the overall ductility content of manufactured hybrid aluminum matrix composites (HAMCs), which significantly enhances the hardness value of manufactured HAMCs. Further, the increased content of combined reinforcement in the matrix alloy leads to increased dislocation densities during solidification because of thermal mismatch of the matrix alloy and reinforcement. The mismatch of thermal expansion between matrix and

reinforcement due to temperature difference results in large internal stresses, due to which the matrix deforms plastically to accommodate the smaller volume expansion of reinforcement particles. Enhancement in dislocation densities at the particle metal interface results in higher resistance to plastic deformation leading to improved hardness. These results are in agreement with the results of Rohatgi *et al.*^[28] The same results of increase in hardness with increasing content of combined reinforcement in the metal matrix irrespective of the manufacturing process of HAMCs were obtained by previous researchers.^[2,3,11,12,14] However, the hardness of hybrid composites is more than that of Gr-reinforced composites and lower than that of Si₃N₄-reinforced composites at all weight percent of reinforcements. This may be due to the less hard Gr particles that are added as second reinforcement in harder Si₃N₄, resulting in intermediate hard hybrid composites.

D. Development of Wear Model by RSM

The central composite design (CCD) is used in this experimental study. Significance testing of the coefficients, acceptability of the wear model, and analysis of variance (ANOVA) was carried out by Design Expert Software to evaluate the significant factors, square terms, and interactions affecting the response (dry sliding wear).

The analysis of variance (ANOVA) has been shown in Table VI. The analysis of variance (ANOVA) shows the significance of various factors and their interactions at 95 pct confidence interval. ANOVA shows the “Wear Model” as “Significant,” while the “Lack of fit” is “Not significant” which are desirable from a model point of view. The probability values <0.05 in the “Prob.>F” column indicate the significant factors and their interactions. The main factors and their interactions are included in the final dry sliding wear model, while the insignificant interactions are excluded from the final dry sliding wear model. Percentage reinforcement (*R*), load (*L*), sliding speed (*S*), and sliding distance (*D*) are the significant individual factors, while load-sliding speed (LS), load-sliding distance (LD), and sliding speed-sliding distance (SD) are the significant interactions among various

process variables and second-order term of load (*L*), sliding speed (*S*), and sliding distance (*D*) are also significant terms which also affect the dry sliding wear.

After eliminating the non-significant terms, the dry sliding wear model generated in terms of coded and actual process variables is given below (Eqs. [1] and [2], respectively):

In coded parameters

$$\begin{aligned} \text{Dry Sliding Wear} = & 8.292 \times 10^{-3} - 9.042 \times 10^{-4} \\ & \times R + 1.263 \times 10^{-3} \times L \\ & - 1.738 \times 10^{-3} \times S + 4.288 \\ & \times 10^{-3} \times D + 4.813 \times 10^{-4} \\ & \times L \times S + 6.813 \times 10^{-4} \times L \\ & \times D - 5.562 \times 10^{-4} \times S \times D \\ & + 4.437 \times 10^{-4} \times R^2 + 4.813 \\ & \times 10^{-4} \times S^2 + 6.938 \times 10^{-4} \times D^2 \end{aligned} \quad [1]$$

In actual parameters

$$\begin{aligned} \text{Dry sliding wear} = & 0.016469 - 8.93056 \times 10^{-4} \\ & \times \text{reinforcement } (R) - 1.48333 \\ & \times 10^{-4} \times \text{load } (L) - 0.011000 \\ & \times \text{sliding speed } (S) - 6.25000 \\ & \times 10^{-7} \times \text{sliding distance } (D) \\ & + 8.02083 \times 10^{-5} \times \text{load}(L) \\ & \times \text{sliding speed}(S) + 1.13542 \times 10^{-7} \\ & \times \text{load}(L) \times \text{sliding distance } (D) \\ & - 3.47656 \times 10^{-6} \times \text{sliding speed } (S) \\ & \times \text{sliding distance } (D) + 4.93056 \\ & \times 10^{-5} \text{reinforcement } (R)^2 \\ & + 3.00781 \times 10^{-3} \\ & \times \text{sliding speed } (S)^2 + 4.33594 \\ & \times 10^{-9} \times \text{sliding distance } (D)^2 \end{aligned} \quad [2]$$

Table VI. ANOVA Table for Wear of Hybrid Composites (After Backward Elimination)

Source	Sum of Squares	DOF	Mean Square	<i>f</i> value	Prob > <i>f</i>
Model	6.083×10^{-4}	10	6.083×10^{-5}	142.83	<0.0001
Reinforcement, R	1.962×10^{-5}	1	1.962×10^{-5}	46.07	<0.0001
Load, L	3.825×10^{-5}	1	3.825×10^{-5}	89.81	<0.0001
Sliding Speed S	7.245×10^{-5}	1	7.245×10^{-5}	170.11	<0.0001
Sliding Distance D	4.412×10^{-4}	1	4.412×10^{-4}	1035.83	<0.0001
Interaction LS	3.706×10^{-6}	1	3.706×10^{-6}	8.7	0.0082
Interaction LD	7.426×10^{-6}	1	7.426×10^{-6}	17.43	0.0005
Interaction SD	4.951×10^{-6}	1	4.951×10^{-6}	11.62	0.0029
Quadratic R ²	5.514×10^{-6}	1	5.514×10^{-6}	12.95	0.0019
Quadratic S ²	6.485×10^{-6}	1	6.485×10^{-6}	15.23	0.001
Quadratic D ²	1.348×10^{-5}	1	1.348×10^{-5}	31.64	<0.0001
Residual	8.093×10^{-6}	19	4.259×10^{-7}		
Lack of Fit	7.179×10^{-6}	14	5.128×10^{-7}	2.81	0.1302
Pure Error	9.133×10^{-7}	5	1.827×10^{-7}		
Cor. Total	6.164×10^{-4}	29			

The R^2 and adjusted R^2 values at 95 pct confidence interval are close to each other, which indicate that the model is statistically significant.

E. Effect of Individual Variables on Wear of Hybrid Composite

The effect of individual factors on dry sliding wear is shown in Figures 3((a) through (d)). The effect of percentage reinforcement (R), load (L), sliding speed (S), sliding distance (D), and that of their interactions on dry sliding wear is given in Eq. [1] which exhibits the dry sliding wear in terms of coded values and Eq. [2] in terms of actual values of factors and their interactions. However, the effects of individual factors are discussed by considering Eq. [1] because all the factors are at same level. The constant 8.292×10^{-3} in the Eq. [1] indicates

the overall average of the dry sliding wear of hybrid composites under all the test conditions. This equation further indicates that the coefficient, 9.042×10^{-4} associated with percentage reinforcement is negative, which signifies a decrease of the wear with an increase of percentage reinforcement (Figure 3(a)). This is attributed to the increase in hardness of the composite with the increasing percentage reinforcement. Increase in hardness of composite lowers the volume of material removed. The effect of load, sliding speed, and sliding distance on the wear is shown in Figures 3((b) through (d)). The coefficients associated with load, sliding speed, and sliding distance are 1.263×10^{-3} , 1.738×10^{-3} , and 4.288×10^{-3} , respectively. This signifies that sliding distance has a more detrimental effect than the applied load on the wear of the hybrid composite. The load determines the contact area and deformation of the material, whereas sliding distance determines the period

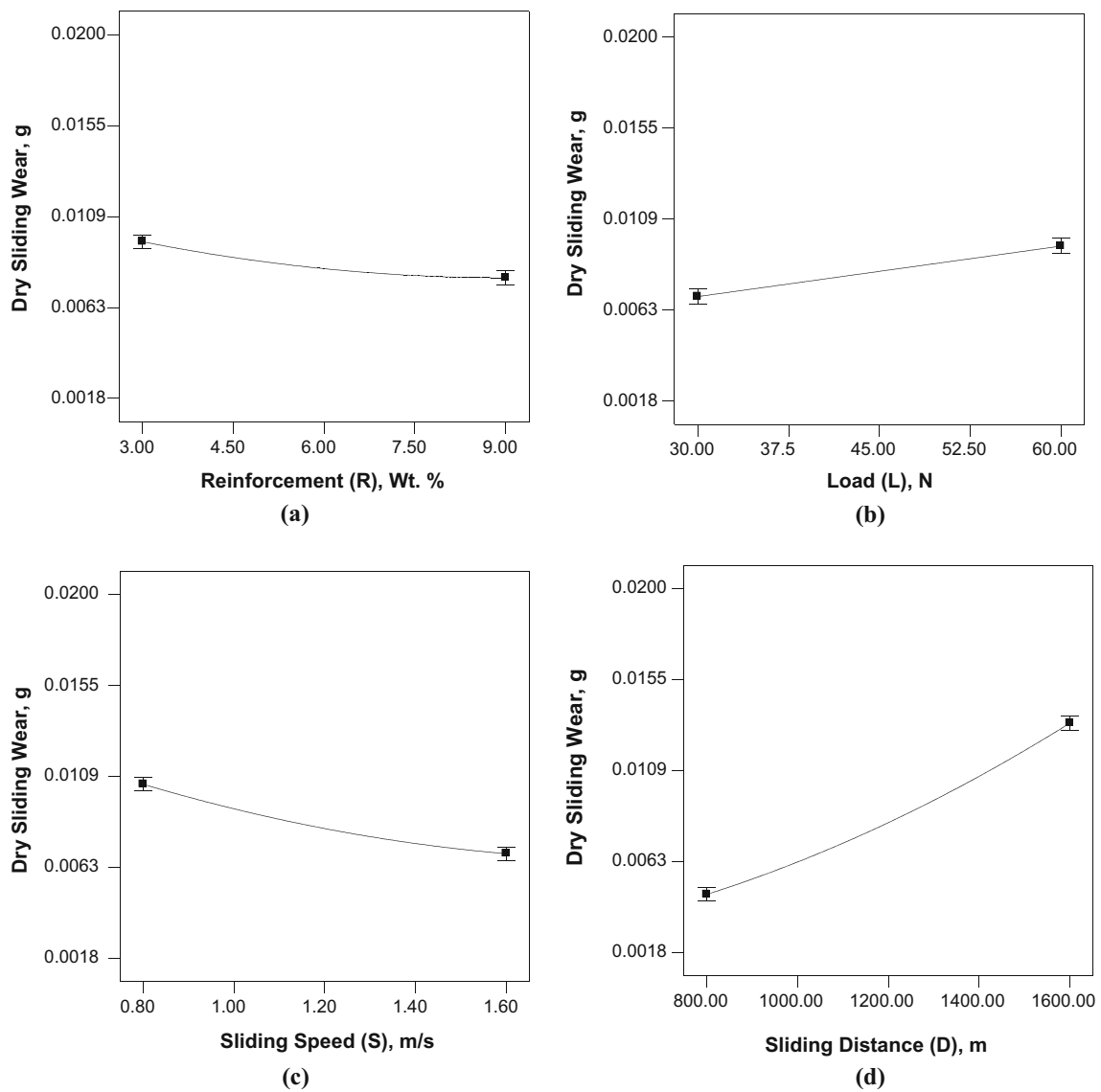


Fig. 3—Effect of individual factors on dry sliding wear (a) reinforcement (R), wt pct (b) load (L), N (c) sliding speed (S), m/s and (d) sliding distance (D), m.

of interaction of wear pins with the counter body. The effect of load on the wear is less as compared to sliding speed and sliding distance. The wear increases with increasing load as shown in Figure 3(b) because load determines the deformation and pressure applied on the contacting surface. The effect of sliding speed on the wear is low as compared to sliding distance as shown in Figure 3(c). The wear decreases with the increase in sliding speed which may be due to the fact that at higher sliding speeds, the time of contact between the sliding surfaces decreases which, in turn, decreases the wear. The effect of sliding distance on the wear is shown in Figure 3(d), the wear increases with the increase in sliding distance because at higher sliding distance, the period of interaction between the sliding surfaces increases, which enhances the wear.

F. Interaction Effect of Different Variables on Wear of Hybrid Composite

Figures 4((a) through (c)) shows the 3-D interaction plots between different wear parameters. Figure 4(a) shows the 3-D interaction plot between load-sliding speed (LS) on wear. The wear has been found to be increased with the increase in load (30 to 60 N) at lower value of sliding speed (0.80 m/s). Also at a larger value of sliding speed (1.6 m/s), the wear increases with the increase in load (30 N) to 60 N). At a lower value of load (30 N), the wear has been found to be decreased with the increase in sliding speed (0.8 to 1.6 m/s). Similarly, the wear also decreases with the increase in sliding speed (0.8 to 1.6 m/s) at a higher value of load (60 N). The main reason behind this is that with the increase in sliding speed, the interaction spell of material decreases,

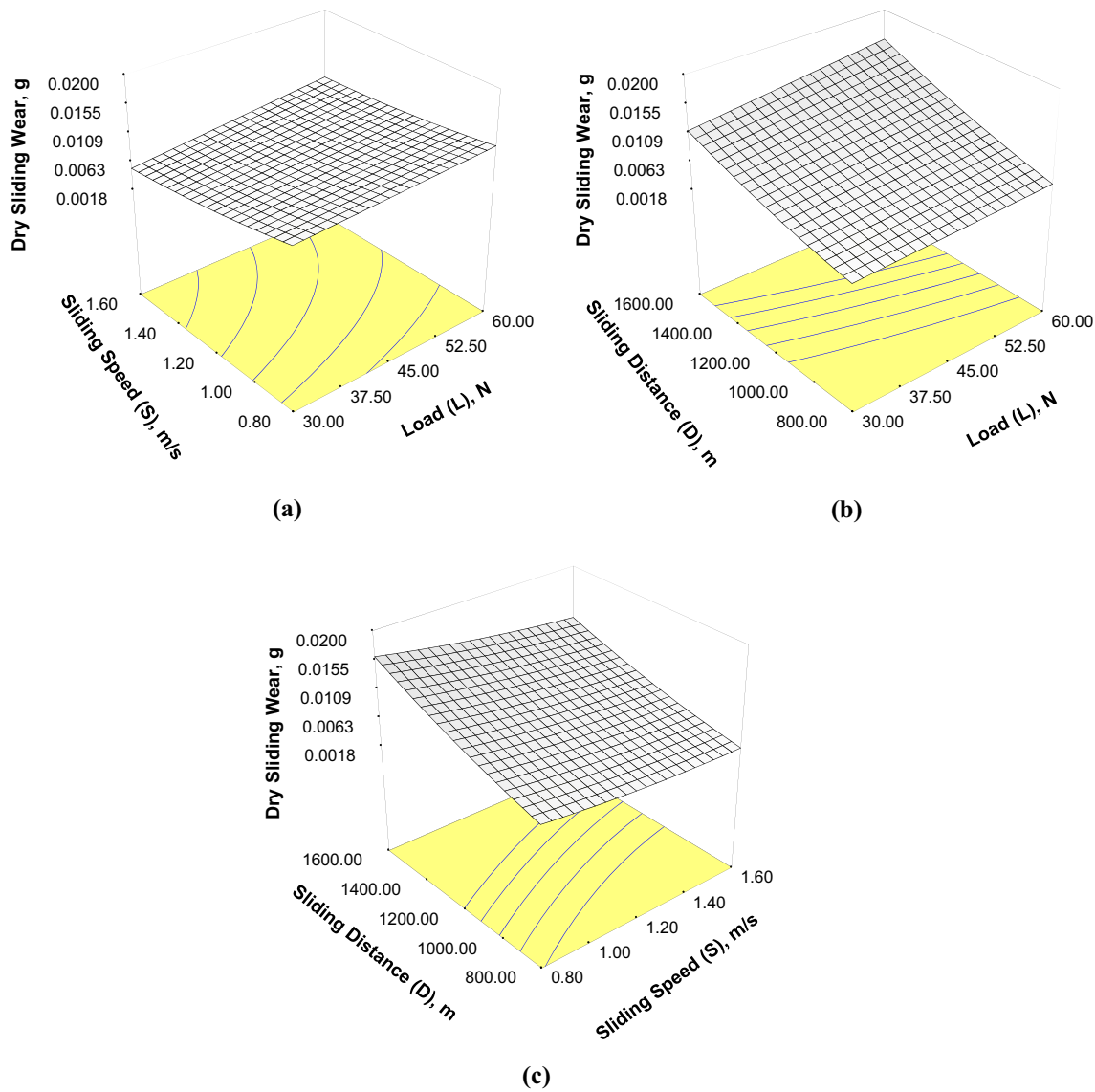


Fig. 4—Effect of interaction on dry sliding wear (a) load-sliding speed (LS), (b) load-sliding distance (LD), and (c) sliding speed-sliding distance (SD).

Table VII. Confirmation Tests and Their Comparison with Experimental Results

Exp. No	Process Parameters				Wear (g)		
	Reinforcement (R), wt pct	Load (L), N	Sliding Speed (S), m/s	Sliding Distance (D), m	Experimental Results	Modeled Results	Error (pct)
1	4.00	55	0.85	1500	0.01645	0.0159	3.34
2	8.00	35	1.5	800	0.0032	0.0030	6.25
3	8.5	50	0.9	900	0.0067	0.0064	4.47

which decreases the wear keeping load at a constant value, which keeps a uniform pressure between the pin and disk. In another case when the load increases and sliding speed is kept constant, then at every point of contact, the pressure between the contact surface increases and results in more wear. In this way, the lower value of load (30 N) and higher value of sliding speed (1.6 m/s) will be auspicious for minimum wear. The collective effect of increase in load-sliding speed (LS) increases the wear of hybrid composites.

The 3-D interaction plot of load-sliding distance (LD) on the wear is shown in Figure 4(b). The wear has been found to be increased with the increase in load (30 to 60 N) at a lower value of sliding distance (800 m). The wear has also been found to be increased with escalation in load (30 to 60 N) at a higher value of sliding distance (1600 m). At a low value of load (30 N), the wear has been found to be increased with the increase in sliding distance (800 to 1600 m). In the same way, wear also increases at a higher value of load (60 N) with the increase in sliding distance (800 to 1600 m). The foremost reason behind this is that with the increase in sliding distance, the contact time between the pin and disk increases, which increases the contact surface and finally wear (load was kept constant at 30 and 60 N, respectively). In another case, when load increases while keeping the sliding distance constant wear increases, which is due to the higher load contact pressure that increases between sliding surfaces, which results in more material removal. The conditions favorable for lowest wear are low value of load (30 N) and sliding distance (800 m). The overall effect of increase in both load and sliding distance increases the wear of hybrid composites.

Figure 4(c) shows the 3-D interaction plot of sliding speed-sliding distance (SD) on wear. The wear decreases with escalation in sliding speed (0.8 to 1.6 m/s) at a smaller value of sliding distance (800 m). Similarly, at an upper value of sliding distance (1600 m) the wear has been found to be decreased with the increase in sliding speed (0.8 to 1.6 m/s). At a lower value of sliding speed (0.8 m/s), the wear has been found to be increased with the increase in sliding distance. Likewise at higher sliding speed (1.6 m/s), the wear increases with the increase in sliding distance (0.8 to 1.6 m/s). This may be due to the fact that with increasing the sliding speed and keeping the sliding distance constant, the time of interaction between the sliding surfaces decreases and at every time a new surface comes in contact which decreases the wear. In contrast to this, the sliding distance increases the wear due to additional contact time between the surfaces. The conditions which favor the minimum or optimum wear are higher value of sliding speed (1.6 m/s) and lower value

of sliding distance (800 m). The cumulative effect of the increase in both sliding speed and sliding distance reduces the wear of hybrid composites.

G. Validity of Wear Model and Confirmation Experiments

The validity of the dry sliding wear model is evaluated by conducting dry sliding wear test on hybrid composites at different levels of the experimental factors such as percentage reinforcement (R), load (L), sliding speed (S), and sliding distance (D). The independent variable selected for the confirmation experiments must lie within the ranges for which the equations are derived. The three confirmation experiments are performed for dry sliding wear at the condition of independent process parameter delivered by quadratic model. The data predicted from developed model and experimental results are compared for confirmation and have been listed in Table VII. The errors between experimental and predicted values are small (3 to 7 pct), which confirm the experimental conclusion.

IV. CONCLUSIONS

The following concluding remarks have been drawn from the present investigation.

1. The AA6082/Si₃N₄, AA6082/Gr, and AA6082 (Si₃N₄ + Gr) hybrid composites are successfully fabricated by stir casting process. Scanning electron micrograph shows a reasonably more uniform distribution of reinforcement particles in case of hybrid composites than that of single reinforced Gr and Si₃N₄ composites.
2. The hardness of hybrid composite increases from 49.5 to 84 VHN, while that of Si₃N₄-reinforced composites from 49.5 to 93.5 VHN, and hardness of Gr-reinforced composites decreases from 49.5 to 44 VHN with respect to weight percent of reinforcement (*i.e.*, from 0 to 12 pct).
3. The Wear resistance of hybrid composites has been found to be improved as compared to conventional AA 6082.
4. The wear of hybrid composites decreases with the increasing sliding speed and percentage reinforcement and increases with the increasing load and sliding distance.
5. The load-sliding distance (LD) shows a more detrimental effect on wear of hybrid composites, as compared to the other two interactions (LS and SD).

6. The model developed with RSM results in good prediction of the wear of hybrid composite within the range of applied factors. The errors between the modeled and experimental results are within 3 to 7 pct.

REFERENCES

1. Y.B. Liu, J.D. Hu, Z.Y. Cao, and P.K. Rohatgi: *Wear*, 1997, vol. 206, pp. 83–86.
2. A.M. Hassan, G.M. Tashtoush, and A.K.J. Ahmed: *J. Compos. Mater.*, 2007, vol. 41, pp. 453–65.
3. F. Akhlaghi and A. Bidaki: *Wear*, 2009, vol. 266, pp. 37–45.
4. G.M.L. Ted and C.Y.A. Tsao: *Compos. Sci. Technol.*, 2000, vol. 60, pp. 65–74.
5. Z.Y. Xiu, G.Q. Chen, Y.M. Liu, W.S. Yang, and G.H. Wu: *Trans. Nonferr. Met. Soc. China*, 2009, vol. 19, pp. 373–77.
6. H. Arik: *Mater. Des.*, 2008, vol. 29, pp. 1856–61.
7. C.S. Ramesh, R. Keshavamurthy, B.H. Channabasappa, and S. Pramod: *Tribol. Int.*, 2010, vol. 43, pp. 623–34.
8. M.H. Song, G.H. Wu, W.S. Yang, W. Jia, Z.Y. Xiu, and G.Q. Chen: *J. Mater. Sci. Technol.*, 2010, vol. 26 (10), pp. 931–35.
9. Z.Y. Xiu, G.Q. Chen, G.H. Wu, W.S. Yang, and Y. Liu: *Trans. Nonferr. Met. Soc. China*, 2011, vol. 21, pp. 285–89.
10. A. Sato and R. Mehrabian: *Metall. Trans. B*, 1976, vol. 7B, pp. 443–51.
11. A.R. Riahi and A.T. Alpas: *Wear*, 2001, vol. 251, pp. 1396–1407.
12. S. Basavarajappa, G. Chandramohan, M. Arjun, T. Mukundan, R. Subramanian, and P. Gopalakrishnan: *Wear*, 2007, vol. 262, pp. 1007–12.
13. P.K. Rohatgi, R. Guo, J.K. Kim, S. Rao, T. Stephenson, and T. Waner: *On Wear of Engineering Materials Proceedings, Indianapolis, Indiana*, 1997, pp. 205–11.
14. S. Suresha and B.K. Sridhara: *Mater. Des.*, 2010, vol. 31, pp. 4470–77.
15. S.A. Alidokht, Z.A. Abdollah, S. Soleymani, and H. Assadi: *Mater. Des.*, 2011, vol. 32, pp. 2727–33.
16. P.K. Rohatgi, Y. Liu, and S. Ray: *ASM Handbook*, Materials Park, ASM International, 2004, vol. 18, pp. 801–11.
17. K. Umanath, K. Palanikumar, and S.T. Selvamani: *Compos. B*, 2013, vol. 53, pp. 159–68.
18. R. Kumar and S. Dhiman: *Mater. Des.*, 2013, vol. 50, pp. 351–59.
19. A. Baradeswaran, S.C. Vettivel, A.E. Perumal, N. Selvakumar, and R.F. Issac: *Mater. Des.*, 2014, vol. 63, pp. 620–32.
20. K. Venkateswarlu, S. Mohapatra, R.G. Rao, A.K. Ray, L.C. Pathak, and D.P. Mondal: *Tribol. Lett.*, 2006, vol. 24, pp. 7–14.
21. J. Hashim, L. Looney, and M.S.J. Hashmi: *J. Mater. Process. Technol.*, 1999, vols. 92–93, pp. 1–7.
22. H. Sevik and K.S. Can: *Mater. Des.*, 2006, vol. 27, pp. 676–83.
23. E.D. Rabinowicz: *Friction and Wear of Work Hardening in the Design of Wear Resistant Materials*, Wiley, New York, 1965, pp. 168–74.
24. C. Suryanarayana: *Prog. Mater. Sci.*, 2001, vol. 46, pp. 1–184.
25. M. Ghaffari, P.Y. Tan, M.E. Oruc, O.K. Tan, M.S. Tse, and M. Shannon: *Catal. Today*, 2011, vol. 161, pp. 70–77.
26. S.M. Nazanin, A.R. Kamali, and R. Mobarra: *Mater. Lett.*, 2010, vol. 64, pp. 309–12.
27. K.B. Anil, J. Konar, S. Kole, and S. Narayanan: *J. Appl. Polym. Sci.*, 1995, vol. 57, pp. 631–37.
28. P.K. Rohatgi, F.M. Yarandi, and Y. Liu: in *Proc. of International Symposium on Advances in Cast Reinforced Metal Composites*, S.G. Fishman and A.K. Dhindra, eds., ASM International Publication, Materials Park, OH, 1988, p. 249.